



# In Vitro Developmental Acceleration of Hippocampal Neurons on Nanostructures of Self-Assembled Silica Beads in Filopodium-Size Ranges\*\*

Kyungtae Kang, Sung-Eun Choi, Hee Su Jang, Woo Kyung Cho, Yoonkey Nam,\*  
Insung S. Choi,\* and Jin Seok Lee\*

The neurite outgrowth and path-finding behaviors of neurons are governed by two protrusive, actin-based molecular structures, filopodia and lamellipodia, the diameter of which is generally in the range of 100–300 nm.<sup>[1]</sup> The dynamic stability of filopodia and lamellipodia allows neuronal cells to recognize the surrounding environments at the nanometer scale and to subsequently modify their cytoskeletal structures in response to stimuli/cues.<sup>[2]</sup> For example, permissive cues impede the retrograde flow of actin filaments and promote their assembly by generating tensions to the filopodia,<sup>[3]</sup> resulting in the overall advance of neurites toward the cues.

Neurons encounter nanotopographical distributions of permissive and non-permissive cues *in vivo*, exemplified by protein structures in the extracellular matrix and tissue scaffolds or external morphologies of supporting cells. Although the surface roughness is known to affect the neuronal behaviors *in vitro* in various aspects, such as attachment and survival,<sup>[4]</sup> axonal guidance,<sup>[5]</sup> and neurite outgrowth,<sup>[6]</sup> there have been few reports on developmental responses of neurons to nanotopographies.<sup>[7,8]</sup> Because the polarized morphology and specialized compartments (e.g., axons and dendrites) of neurons are crucial and decisive

characteristics for neuronal activities, it is much more beneficial to the precise control of neuron/materials interfaces to manipulate neuronal development and neurite outgrowth than to do general behaviors, such as attachment and survival. The concrete understanding of nanotopographical effects also would contribute to the biomedical applications, which demand the controlled development or regeneration of nerve systems at a certain position towards a pre-determined direction, as well as to fundamental studies on nanotopographical role for neuronal development *in vivo*.<sup>[9]</sup>

To understand the function of filopodia as an antenna for the environmental exploration,<sup>[2]</sup> it is necessary to investigate the developmental responses of neurons to nanostructures, the feature size of which is comparable to that of filopodia (100–300 nm). Herein, we systematically varied the feature sizes of nanostructures by organizing spherical nanoparticles with different diameters on a glass substrate, and found that the neuritogenic acceleration of hippocampal neurons occurred on the nanostructures the period of which was larger than 200 nm.


For the generation of nanosurfaces with various feature sizes, silica beads with the diameters ranging from 100 to 700 nm were synthesized by hydrolysis of tetraethyl orthosilicate.<sup>[10]</sup> The diameter was controlled to be 110, 190, 320, 480, or 670 nm by changing the re-growth cycles of seeds and the concentrations of reactants (See the Supporting Information for the experimental details; Figure S1). The silica beads were denoted as SB-110, SB-190, SB-320, SB-480, and SB-670, respectively. Among the methods for organizing nano-sized beads into two-dimensional arrays on a solid substrate,<sup>[11]</sup> rubbing was reported to be a highly effective in the monolayer assembly with the precise control of the interparticle distance, and simple, fast, and reproducible on a large area (Figure 1a).<sup>[12]</sup> Figure 1b shows the SEM images of the bead monolayers with the different diameters, formed by the rubbing method. This simple method yielded high-quality monolayers with uniform interparticle distance regardless of the bead diameters. To prevent the undesired detachment of silica beads from the surface during cell culture, we baked the substrate at 350 °C for 3 h (see the Supporting Information, Figure S2, for the experimental details). Figure 1c shows a representative SEM image of a hippocampal neuron cultured on a monolayer of SB-110, where the beads are smaller than the filopodia.

The surface of silica beads was made to be neuron-adhesive by 2 min-O<sub>2</sub>-plasma treatment, followed by 1 h dipping in aqueous poly-D-lysine solution (0.1 mg mL<sup>-1</sup> in

[\*] K. Kang,<sup>[†]</sup> Dr. W. K. Cho, Prof. Dr. I. S. Choi  
Molecular-Level Interface Research Center, Department of Chemistry, KAIST  
Daejeon 305-701 (Korea)  
E-mail: ischoi@kaist.ac.kr  
Homepage: <http://cisgroup.kaist.ac.kr>  
Prof. Dr. Y. Nam, Prof. Dr. I. S. Choi  
Department of Bio and Brain Engineering, KAIST  
Daejeon 305-701 (Korea)  
E-mail: ynam@kaist.ac.kr  
Homepage: <http://neuros.kaist.ac.kr>  
S.-E. Choi,<sup>[†]</sup> H. S. Jang, Prof. Dr. J. S. Lee  
Department of Chemistry, Sookmyung Women's University  
Seoul 140-742 (Korea)  
E-mail: jinslee@sookmyung.ac.kr  
Homepage: <http://sookmyung.ac.kr/~FETNS>

[†] These authors contributed equally to this work.

[\*\*] This work was supported by the Korea Research Foundation Grant funded by the Korean Government (MOEHRD, KRF-2008-313-d00614) and the Basic Science Research Programs through the National Research Foundation of Korea (NRF) funded by the Ministry of Education, Science and Technology (2011-0001318, 2009-0077751, 2009-0080081, and 2010-0025065) and the Brain Research Center of the 21st Century Frontier Research Program.

 Supporting information for this article is available on the WWW under <http://dx.doi.org/10.1002/anie.201106271>.

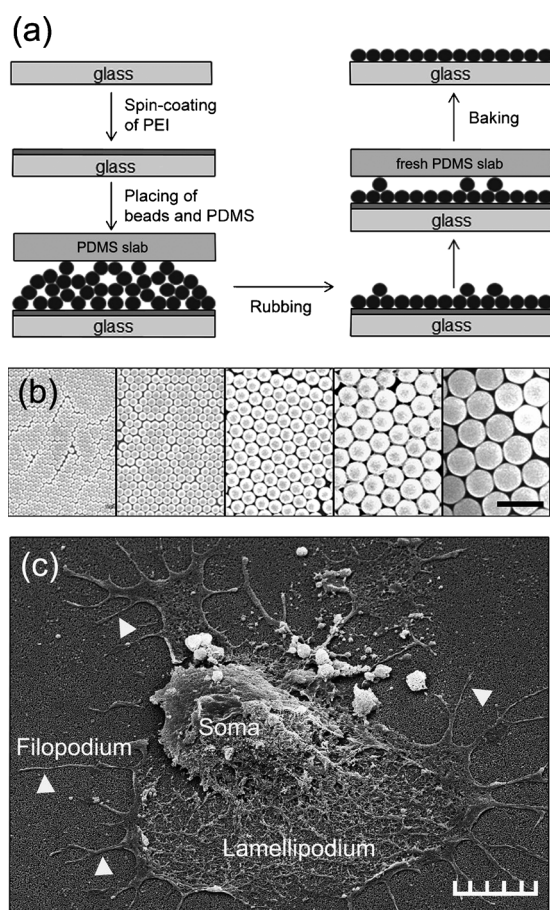


**Figure 1.** a) A schematic illustration of the formation of two-dimensional nanostructures of silica beads on a glass substrate. b) SEM images of the nanostructures assembled with SB-110, SB-190, SB-320, SB-480, and SB-670 (from left to right). The scale bar is 1  $\mu\text{m}$ . c) SEM image of a neuron at 1 DIV cultured on SB-110. The scale bar is 5  $\mu\text{m}$ . The arrowheads indicate filopodia.

deionized water). Hippocampal neurons were then plated at the density of 50 cells/ $\text{mm}^2$ . Figure 2a shows phase-contrast optical images of the neurons at 1 DIV (day in vitro) and 2 DIV. Based on neuronal morphologies, the substrates were categorized into two groups: Group-I (SB-110 and SB-190) and Group-II (SB-320, SB-480, and SB-670). We observed noticeable differences in neuronal development between the two groups even at 1 DIV. In Group-I, most of neurons had either lamellipodia or short minor neurites at 1 DIV, and the ratio between neurons with and without neurites was about 4:6. This ratio was similar to neurons grown on a polylysine-treated glass coverslip at 1 DIV.<sup>[13]</sup> In a stark contrast, more than 80% of Group-II neurons had neurites at 1 DIV, and the length of the neurites was significantly longer than that of Group-I neurons. In terms of axonal development, more neurons in Group-II had a major neurite (“putative” axon) than those in Group-I, which implied that axonal polarization processes were more active on Group-II substrates than Group-I substrates. At 2 DIV, Group-II neurons had one long branching axon and a few minor neurites, which was a phenotype of cultured hippocampal neurons.<sup>[13]</sup> The immu-

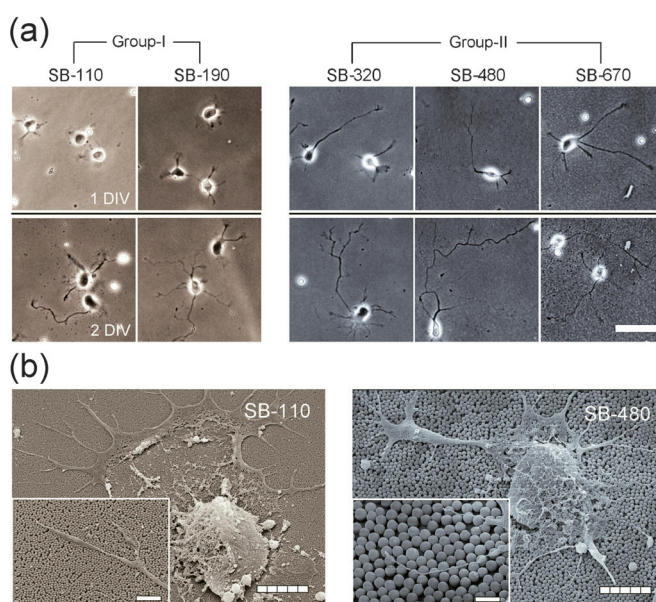


**Figure 2.** a) Phase-contrast optical micrographs of hippocampal neurons cultured on bead-packed substrates. The scale bar is 50  $\mu\text{m}$ . b) SEM images of the hippocampal neurons on SB-110 (left) and SB-480 (right). The scale bar is 5  $\mu\text{m}$ . Insets: Magnified images of filopodial tips. The scale bar is 1  $\mu\text{m}$ . The original gray images were rendered with a monochromatic color for the comparison between the groups.

nostaining showed that the microtubules and filopodial/lamellipodial structures were well-developed on all the bead substrates (See the Supporting Information; Figure S3). These results were in a good agreement with our previous report: the developmental acceleration occurred on a 400 nm-pitched anodized aluminum oxide substrate.<sup>[8]</sup>

Scanning electron microscopy (SEM) was used to examine the physical interactions of neurons with silica beads. The bead size seemed to affect the filopodial contact with the substrate in a different fashion: filopodia of the neurons in Group-I extended straight regardless of the bead curvature, while filopodia in Group II did not grow straight and seemed to have many interactions with surface structures such as trenches, bead surfaces, and gaps between the beads (Figure 2b, insets). The SEM micrographs showed that different bead sizes caused the different spatial distribution of interaction spots between the filopodia and the substrate. These interactions were believed to be phenomenologically different from the ones with microstructures. Microtopographies, such as microchannels and micropillar array with feature sizes larger than 1  $\mu\text{m}$ ,<sup>[4–6]</sup> were reported to have influences on neuronal growth directly at cellular scale; entire neurites were trapped within the microstructures, which physically restricted the direction of neurite growth or generated cellular-scale tensions.<sup>[5,6]</sup> In contrast, nanotopographies would have localized effects on subcellular structures such as filopodia, amplified to the cellular-scale responses such as developmental acceleration. Our results supports the idea that nanotopographical features trigger intracellular signaling pathways through mechanotransductions of cytoskeletal structures, and the discontinuous or jumping stimuli of

adhesion bigger than the size of filopodia would change the developmental characteristics of neurons.

To investigate neuritogenesis between the groups (Group-I and Group-II) further, we cultured neurons on coverslips and classified them into three developmental stages:<sup>[8,13]</sup> lamellipodia form around the soma (stage 1); the lamellipodia coalesce at several discrete sites around the cell periphery, where minor neurites begin to extend with growth cones at their ends (stage 2); one neurite (major neurite) grows two- or three-times longer than the others, and cell morphology is polarized (stage 3). Figure 3a clearly shows the differences in

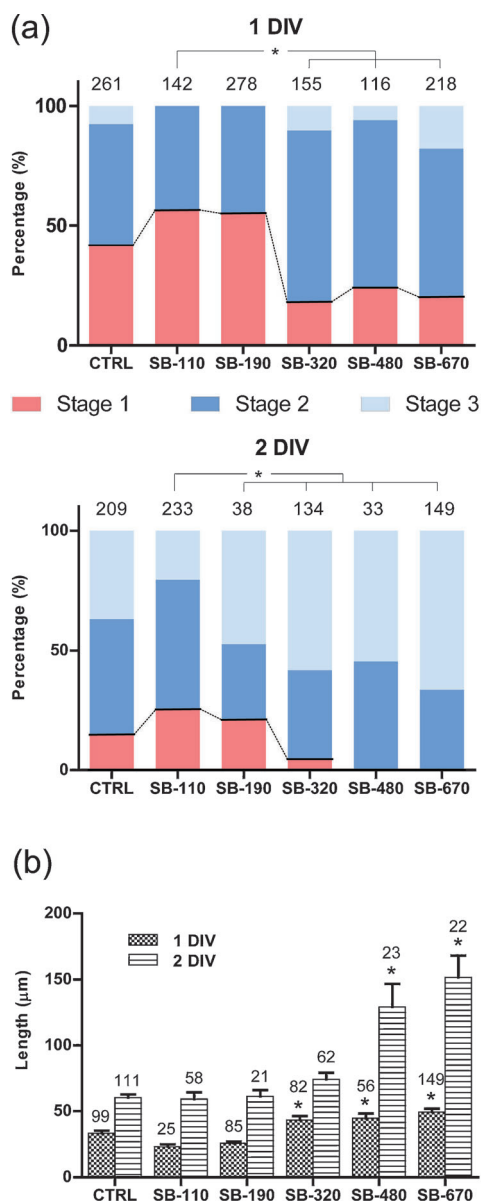


**Figure 3.** a) Percentages of neurons in each stage at 1 DIV and 2 DIV. The results from the substrates were compared with SB-110 by the chi-square test. There was a significant difference ( $*p < 0.001$ ). b) Average length ( $\pm$  standard error) of major neurites. All substrates were compared with SB-110 by one-way ANOVA at the significant level of 99%, followed by the Bonferroni's multiple comparison test ( $*p < 0.001$ ). The numbers indicate data points for the statistics. CTRL: poly-D-lysine-coated coverslips.

distribution of neuronal populations in the two groups. In Group-I, more than 50% of the neurons belonged to stage 1 at 1 DIV, while more than 75% of the neurons in Group-II were already at stage 2 or 3. At 2 DIV, few neurons in Group-II remained in stage 1 (4, 0, and 0% for SB-320, SB-480, and SB-670, respectively), and many neurons populated more at stage 3 (58, 54, and 66%). The neurons in Group-I were also developed, but the percentage of the neurons in stage 1 was still 21–25% at 2 DIV. The length of the longest major neurite also showed similar bimodal distribution (Figure 3b). At 1 DIV, the average length for Group-II was 44–49  $\mu\text{m}$ , while that for Group-I was 23–25  $\mu\text{m}$ . The length difference became much larger at 2 DIV: 151.8  $\pm$  16.5  $\mu\text{m}$  for SB-670, 129.2  $\pm$  17.6  $\mu\text{m}$  for SB-480, 74.3  $\pm$  4.9  $\mu\text{m}$  for SB-320, 61.2  $\pm$  4.8  $\mu\text{m}$  for SB-190, and 59.3  $\pm$  5.1  $\mu\text{m}$  for SB-110. Although the length for SB-320 was relatively short, it was still longer than that for Group-I. Taken together, the results indicated that neurons sprouted neurites faster, and the polarization process was also accelerated on the substrates with beads larger than 200 nm in diameter. The neurons sensed the nanostructures differently and behaved differently with a threshold of about 200–300 nm.

To examine the importance of filopodia in sensing nanotopographical differences, we treated neurons with cytochalasin D, an F-actin-depolymerization agent, while they were cultured on silica beads (Figure 4a). Cytochalasin D has been shown to be effective in disrupting F-actin-based structures of hippocampal neurons, such as filopodia, generating elongated

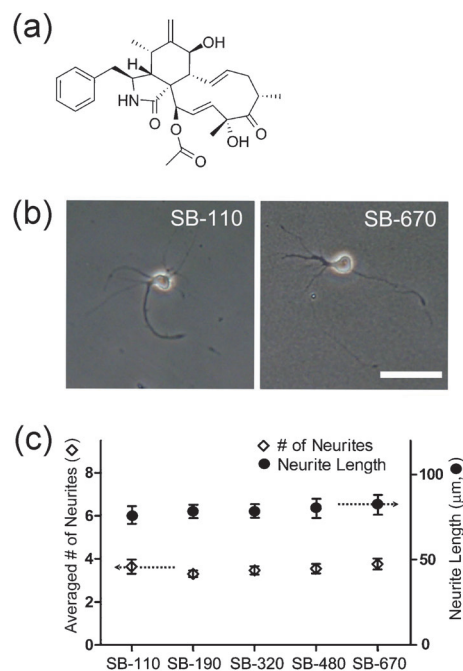


**Figure 4.** a) Chemical structure of cytochalasin D. b) Phase-contrast micrographs of hippocampal neurons cultured on bead-packed substrates (SB-110 and SB-670) with the treatment of cytochalasin D. The scale bar is 50  $\mu\text{m}$ . c) Quantitative analyses of the longest-neurite lengths and the average number of neurites. There were no significant differences between any pair of them for both graphs ( $N = 26, 60, 36, 25,$  and  $30$  for the number of neurites, and  $27, 66, 33, 29,$  and  $40 \mu\text{m}$  for the neurite lengths; mean  $\pm$   $\sigma$ ).

neurites and multiple axons.<sup>[14]</sup> We added cytochalasin D to the culture media (final concentration: 1  $\mu\text{M}$ ) immediately after seeding, and cultured neurons for 1 day. Interestingly, we did observe the same phenotype for all the substrates including the glass control: treated with cytochalasin D, neurons exhibited elongated, multiple, thin, and curved neurites at 1 DIV (Figure 4b for representative images for SB-110 and SB-670). In addition, there was no significant difference in both the length of the major neurite and the number of the neurites (Figure 4c). The results implied that filopodia were essential for the observed, different responses of hippocampal neurons toward nanotopographical surface features.

In summary, we showed that the developmental acceleration of hippocampal neurons occurred on the well-packed structures of silica beads bigger than 200 nm in diameter. The biochemical inhibition of filopodia formation suggested that neurons sensed nanotopographies through filopodial activities, which in turn modulated intracellular cytoskeletal dynamics, just as they sense the biochemical cues. Our results also imply that nanotopographical cues are an important feature for guiding neurites during the neural developments in vivo. We believe that this work would provide fundamental but crucial information for studying nanotopographical manipulation of neuronal development, and also be useful for designing sophisticated neural interfaces in neural tissue engineering and others.

### Experimental Section

**Cell Culture:** Primary hippocampal neurons were cultured in serum-free condition. Hippocampus from E-18 Sprague-Dawley rat was triturated in 1 mL of Hank's Balanced Salt Solution (HBSS) using a fire-polished Pasteur pipette. The cell suspension was centrifuged for 2 min at 1000 rpm, and a cell pellet was extracted. The cell pellet was suspended in Neurobasal media supplemented with B-27, 2 mM L-glutamine, 12.5  $\mu\text{M}$  L-glutamic acid, and Penicillin-Streptomycin. Dissociated cells were seeded at the density of 50 cells  $\text{mm}^{-2}$  on a silica bead-assembled substrate. Cultures were maintained in an incubator (5%  $\text{CO}_2$  and 37  $^\circ\text{C}$ ), and a half of media was replaced with fresh culture media without L-glutamic acid supplement every 3–4 days. This study was approved by IACUC (Institutional Animal Care and Use Committee) of KAIST.

**Instruments and Characterizations:** The surface topography of the prepared substrates was investigated by field-emission scanning electron microscopy (FE-SEM; Hitachi S-4800). Before FE-SEM imaging, the cultured substrates were coated with platinum (30 mA, 360 s). Fluorescence micrographs of neuron cultures were obtained using Olympus BX51M (Olympus Corp.) equipped with a CCD camera (DP71, Olympus Corp.). From the images, the lengths of major neurites were measured with Neuron J plugin in Image J software (NIH).

Received: September 5, 2011

Revised: October 7, 2011

Published online: November 25, 2011

**Keywords:** axon outgrowth · cytoskeletal proteins · nanostructures · neurochemistry · silica bead

- [1] P. K. Mattila, P. Lappalainen, *Nat. Rev. Mol. Cell Biol.* **2008**, *9*, 446–454.
- [2] a) F. Polleux, W. Snider, *Cold Spring Harbor Perspect. Biol.* **2010**, *2*, a001925; b) D. A. Fletcher, R. D. Mullins, *Nature* **2010**, *463*, 485–492; c) C. Conde, A. Caceres, *Nat. Rev. Neurosci.* **2009**, *10*, 319–332.
- [3] L. A. Lowery, D. Van Vactor, *Nat. Rev. Mol. Cell Biol.* **2009**, *10*, 332–343.
- [4] a) V. Brunetti, G. Maiorano, L. Rizzello, B. Sorce, S. Sabella, R. Cingolani, P. P. Pompa, *Proc. Natl. Acad. Sci. USA* **2010**, *107*, 6264–6269; b) W. Hällström, T. Mårtensson, C. Prinz, P. Gustavsson, L. Montelius, L. Samuelson, M. Kanje, *Nano Lett.* **2007**, *7*, 2960–2965; c) J. M. Bruder, A. P. Lee, D. Hoffman-Kim, *J. Biomater. Sci. Polym. Ed.* **2007**, *18*, 967–982.
- [5] a) L. Yao, S. Wang, W. Cui, R. Sherlock, C. O'Connell, G. Damodaran, A. Gorman, A. Windebank, A. Pandit, *Acta Biomater.* **2009**, *5*, 580–588; b) A. Ferrari, M. Cecchini, A. Dhawan, S. Micera, I. Tonazzini, R. Stabile, D. Pisignano, F. Beltram, *Nano Lett.* **2011**, *11*, 505–511; c) F. Johansson, P. Carlberg, N. Danielsen, L. Montelius, M. Kanje, *Biomaterials* **2006**, *27*, 1251–1258; d) D. Y. Fozdar, J. Y. Lee, C. E. Schmidt, S. Chen, *Biofabrication* **2010**, *2*, 035005; e) A. Rajniecek, S. Britland, C. McCaig, *J. Cell Sci.* **1997**, *110*(Pt 23), 2905–2913; f) N. M. Dowell-Mesfin, M. A. Abdul-Karim, A. M. Turner, S. Schanz, H. G. Craighead, B. Roysam, J. N. Turner, W. Shain, *J. Neural Eng.* **2004**, *1*, 78–90.
- [6] N. Gomez, Y. Lu, S. Chen, C. E. Schmidt, *Biomaterials* **2007**, *28*, 271–284.
- [7] a) C. C. Gertz, M. K. Leach, L. K. Birrell, D. C. Martin, E. L. Feldman, J. M. Corey, *Dev. Neurobiol.* **2010**, *70*, 589–603; b) H. Hu, Y. Ni, V. Montana, R. C. Haddon, V. Parpura, *Nano Lett.* **2004**, *4*, 507–511; c) M. J. Jang, S. Namgung, S. Hong, Y. Nam, *Nanotechnology* **2010**, *21*, 235102.
- [8] W. K. Cho, K. Kang, G. Kang, M. J. Jang, Y. Nam, I. S. Choi, *Angew. Chem.* **2010**, *122*, 10312–10316; *Angew. Chem. Int. Ed.* **2010**, *49*, 10114–10118.
- [9] a) N. Y. Harel, S. M. Strittmatter, *Nat. Rev. Neurosci.* **2006**, *7*, 603–616; b) D. Hoffman-Kim, J. A. Mitchel, R. V. Bellamkonda, *Annu. Rev. Biomed. Eng.* **2010**, *12*, 203–231.
- [10] a) W. Stöber, A. Fink, E. Bohn, *J. Colloid Interface Sci.* **1998**, *26*, 62–69; b) K. D. Hartlen, A. P. T. Athanasopoulos, V. Kitaev, *Langmuir* **2008**, *24*, 1714–1720; c) T. Yokoi, Y. Sakamoto, O. Terasaki, Y. Kubota, T. Okubo, T. Tatsumi, *J. Am. Chem. Soc.* **2006**, *128*, 13664–13665.
- [11] a) P. Jiang, M. J. McFarland, *J. Am. Chem. Soc.* **2004**, *126*, 13778–13786; b) S. Wong, V. Kitaev, G. A. Ozin, *J. Am. Chem. Soc.* **2003**, *125*, 15589–15598; c) R. Micheletto, H. Fukuda, M. Ohtsut, *Langmuir* **1996**, *11*, 3333–3336; d) P. Jiang, J. F. Bertone, K. S. Hwang, V. L. Colvin, *Chem. Mater.* **1999**, *11*, 2132–2140.
- [12] a) J. S. Lee, J. H. Kim, Y. J. Lee, N. C. Jeong, K. B. Yoon, *Angew. Chem.* **2007**, *119*, 3147–3150; *Angew. Chem. Int. Ed.* **2007**, *46*, 3087–3090; b) N. N. Khanh, K. B. Yoon, *J. Am. Chem. Soc.* **2009**, *131*, 14228–14230.
- [13] S. Kaech, G. Banker, *Nat. Protoc.* **2006**, *1*, 2406–2415.
- [14] F. Bradke, C. G. Dotti, *Science* **1999**, *283*, 1931–1934.